

Article

# Application of $\beta$ -Phosphorylated Nitroethenes in [3+2] Cycloaddition Reactions Involving Benzonitrile N-Oxide in the Light of a DFT Computational Study

Karolina Zawadzińska and Karolina Kula \* 

Department of Organic Chemistry and Technology, Cracow University of Technology, Warszawska Street, 24, 31-155 Cracow, Poland; karolina.zawadzinska@doktorant.pk.edu.pl

\* Correspondence: kkula@chemia.pk.edu.pl

**Abstract:** The regiochemistry of [3+2] cycloaddition (32CA) processes between benzonitrile N-oxide **1** and  $\beta$ -phosphorylated analogues of nitroethenes **2a–c** has been studied using the Density Functional Theory (DFT) at the M062X/6-31+G(d) theory level. The obtained results of reactivity indices show that benzonitrile N-oxide **1** can be classified both as a moderate electrophile and moderate nucleophile, while  $\beta$ -phosphorylated analogues of nitroethenes **2a–c** can be classified as strong electrophiles and marginal nucleophiles. Moreover, the analysis of CDFT shows that for [3+2] cycloadditions with the participation of  $\beta$ -phosphorylated nitroethene **2a** and  $\beta$ -phosphorylated  $\alpha$ -cyanonitroethene **2b**, the more favored reaction path forms 4-nitro-substituted  $\Delta^2$ -isoxazolines **3a–b**, while for a reaction with  $\beta$ -phosphorylated  $\beta$ -cyanonitroethene **2c**, the more favored path forms 5-nitro-substituted  $\Delta^2$ -isoxazoline **4c**. This is due to the presence of a cyano group in the alkene. The CDFT study correlates well with the analysis of the kinetic description of the considered reaction channels. Moreover, DFT calculations have proven the clearly polar nature of all analyzed [3+2] cycloaddition reactions according to the polar one-step mechanism.



**Citation:** Zawadzińska, K.; Kula, K. Application of  $\beta$ -Phosphorylated Nitroethenes in [3+2] Cycloaddition Reactions Involving Benzonitrile N-Oxide in the Light of a DFT Computational Study. *Organics* **2021**, *2*, 26–37. <https://doi.org/10.3390/org2010003>

Academic Editor: Pierluca Galloni  
Received: 12 January 2021  
Accepted: 4 February 2021  
Published: 16 February 2021

**Publisher's Note:** MDPI stays neutral with regard to jurisdictional claims in published maps and institutional affiliations.



**Copyright:** © 2021 by the authors. Licensee MDPI, Basel, Switzerland. This article is an open access article distributed under the terms and conditions of the Creative Commons Attribution (CC BY) license (<https://creativecommons.org/licenses/by/4.0/>).

**Keywords:** benzonitrile N-oxide;  $\beta$ -phosphorylated nitroethenes; [3+2] cycloaddition reaction; regioselectivity; Density Functional Theory

## 1. Introduction

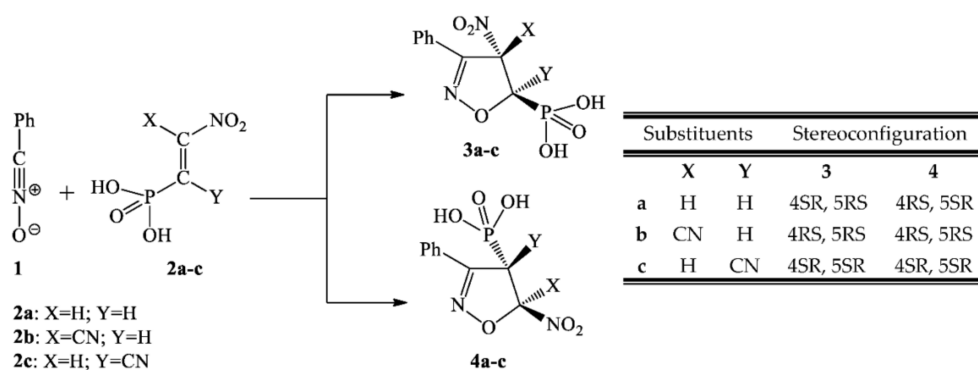
The [3+2] cycloadditions (32CA) are all-purpose strategies to the regio- and stereoselective synthesis of five-membered heterocyclic molecular systems [1–4]. These types of reactions generally proceed under mild conditions, without the presence of catalysts, giving high yields of target compounds [2–4]. Furthermore, 32CA are realized with “full atomic economy.” It is particularly important for the green chemistry aspect [5]. Due to the listed advantages, 32CA are increasingly used by experimental chemists, mainly because of the possibility for using heterocyclic compounds in pharmacology [3,6,7]. The application of 32CA for synthesis has also increased interest among researchers in the theoretical sciences. Research of 32CA via the quantum-chemical calculations enables not only the design of appropriate reaction conditions, but also gives information on the selectivity of these processes [8,9].

As one of the many three atoms components (TACs) used in [3+2] cycloadditions, nitrile N-oxides have a wide application [10]. Reactions between nitrile N-oxides and alkenes obtain  $\Delta^2$ -isoxazolines, which are widely spread out as biological and pharmacological substances. They exhibit, for example, an antibacterial [11] and an antiviral [12] effect; therefore, they can be used in medicine as anti-inflammatory [13,14] and analgesic drugs [15]. The most popular medicines containing isoxazolines rings in their structures are Zonisamid and Risperidone [16]. They can also be successfully used as antipsychotic therapy drugs for the treatment of schizophrenia, bipolar disorder and irritability associated with autism [17]. Industrially, isoxazolines can also be successfully applied as dyes,

agrochemical substances, electrical insulating oils and high temperature lubricants [18]. Moreover, isoxazolines are extremely valuable in organic synthesis. They can be valuable precursors for the synthesis of many versatile compounds, such as  $\alpha,\beta$ -unsaturated ketones,  $\beta$ -hydroxyketones, nitriles, oximes and also  $\beta$ -amino acids and they are also substrates to obtain azaheterocycles [19–21].

In the present paper, we carried out theoretical experiments exploring the possibility of the synthesis of isoxazolines functionalized by a nitro and phosphate group. The possibility of attaching both of these groups in a one-step process provides the 32CA reactions between nitrile N-oxide and phosphorylated analogues of nitroethene. The presence in the molecular structures of nitro and phosphonate groups significantly increases the application spectrum of these compounds and also their further modification, which could be obtained in such reactions as: cycloaddition via *Nef* reaction [22], the *Mukaiyama* reaction [23] or the *Henry* reaction [22]. Moreover, the presence of a nitro group in the compound has the ability to stimulate biological properties of the molecule [24]. The phosphorus atom and phosphate group play a main role in the biochemistry of living, not only because 9% of nucleic acids consist of phosphorus, but also because they appeared to have a great impact on the enzyme activity. For instance, thanks to certain phosphate groups, proteins can carry out particular processes in cells [25,26].

We decided to use a benzonitrile N-oxide **1** as the model TAC. This TAC has been a very popular component in 32CAs, both in experimental research [27,28] and for theoretical research [29,30]. As a dipolarophile, we selected  $\beta$ -phosphoryl nitroethene **2a** and its corresponding  $\alpha$ - and  $\beta$ -cyano analogues **2b** and **2c**. The cyano group in **2a** allows research into the effect of the electron-withdrawing characteristics of conjugated nitroalkenes and its influence on the activation of nitrovinyl moiety. For these defined addends, the [3+2] cycloaddition may theoretically proceed via two competitive channels, giving 4- and 5-nitro-substituted  $\Delta^2$ -isoxazolines (**3a–c** and **4a–c**) (see Scheme 1).



**Scheme 1.** Theoretically possible reaction paths of [3+2] cycloaddition between benzonitrile N-oxide **1** and  $\beta$ -phosphorylated analogues of nitroethenes **2a–c**.

It should be underlined that the molecular mechanism of the presented reaction cannot be defined a priori. For 32CAs, several more mechanisms are possible, e.g., non-polar mechanisms, including synchronous mechanisms, a biradical one-step mechanism and a stepwise biradical mechanism [31], as well as polar mechanisms, including synchronous mechanisms, a one-step-two-stage mechanism or a stepwise zwitterionic mechanism [32,33]. It is impossible to predict the relevant mechanism a priori without any data, which are obtained in the practice. We hope that our study will provide a better understanding of intermolecular interactions of addends and the probable selectivity and the mechanism created by these heterocyclic organic compounds, especially for synthetic chemists.

## 2. Computational Details

All calculations associated with the [3+2] cycloaddition were performed using the GAUSSIAN 09 package [34] in the Prometheus computer cluster of the CYFRONET regional computer center in Cracow. All stationary points were optimized using the M062X functional [35], together with the 6-31+G(d) basis set. This theory level has been commonly used for the mechanistic research aspects of 32CA reactions [8,36–39].

The optimizations of stationary points were carried out using vibrational analysis. For the structure optimization of the molecules, the *Berny* algorithm [40,41] was used. It was found that starting molecules as well as products had positive Hessian matrices. The transition states showed only one negative eigenvalue in their diagonalized Hessian matrices, and their associated eigenvectors were confirmed to correspond to the motion along the reaction coordinate under consideration. For all optimized transition states, intrinsic reaction coordinate (IRC) [42] calculations have been performed to verify if the located TSs are associated with the corresponding minimum stationary points connected to substrates and products.

Calculations of all critical structures were performed for a temperature  $T = 298$  K and pressure  $p = 1$  atm. The solvent effects were simulated using a relatively simple self-consistent reaction field (SCRF) [43,44] based on the polarizable continuum model (PCM) [45].

The global electron density transfer (GEDT) [46] values were designated based on the formula:  $\text{GEDT} = + \sum q_A$ , where  $q_A$  is the net Mulliken charge, and the sum is performed over all the atoms of benzonitrile N-oxide **1**.

In turn, the  $\sigma$ -bond development ( $l$ ) indices were designated based on the formula [47]:

$$l_{X-Y} = 1 - \frac{r_{X-Y}^{\text{TS}} - r_{X-Y}^{\text{P}}}{r_{X-Y}^{\text{P}}}$$

where  $r_{X-Y}^{\text{TS}}$  is the distance between the reaction centers X and Y in the structure of transition state and  $r_{X-Y}^{\text{P}}$  is the same distance in the corresponding product.

Global electronic properties of used addends were estimated based on the equations defined on the basis of conceptual Density Functional Theory (CDFT) based on the equations recommended by *Parr* [48] and *Domingo* [49,50]. The calculation used the functional B3LYP on the basis set 6-31G(d) in the gas phase [49–51].

The electronic chemical potentials ( $\mu$ ) and chemical hardness ( $\eta$ ) were evaluated in terms of one-electron energies of FMO ( $E_{\text{HOMO}}$  and  $E_{\text{LUMO}}$ ) using the following equations [49,52]:

$$\mu \approx \frac{E_{\text{HOMO}} + E_{\text{LUMO}}}{2} \quad \eta \approx E_{\text{HOMO}} - E_{\text{LUMO}}$$

where  $E_{\text{HOMO}}$  and  $E_{\text{LUMO}}$  can be defined as terms of the one-electron energies of the frontier MoS, respectively HOMO and LUMO. The obtained values of  $\mu$  and  $\eta$  were next used to approach a global electrophilicity  $\omega$  based on the formula [48,49]:

$$\omega = \frac{\mu^2}{\eta}$$

In turn, the global nucleophilicity  $N$  can be expressed as [50]:

$$N = E_{\text{HOMO}} - E_{\text{HOMO (TCE)}}$$

where  $E_{\text{HOMO (TCE)}}$  is HOMO energy for tetracyanoethylene (TCE) is the reference value because it presents the lowest HOMO ( $E_{\text{HOMO (TCE)}} = -9.368$  eV).

The local electrophilicity ( $\omega_k$ ) and the local nucleophilicity ( $N_k$ ) focused on atom  $k$  was designated based on global properties and using the *Parr* function ( $P_k^+$  or  $P_k^-$ ), based on the formulas [53]:

$$\omega_k = P_k^+ \cdot \omega \quad N_k = P_k^- \cdot N$$

### 3. Results and Discussion

Our theoretical study was divided into three parts: (i) firstly, the analysis of the electronic properties of addends and their intermolecular interactions according to Conceptual Density Functional Theory (CDFT) reactivity indices was carried out; (ii) in the next paragraph, reaction profiles of [3+2] cycloaddition between benzonitrile N-oxide **1** and  $\beta$ -phosphorylated analogues of nitroethenes **2a–c** are explored and characterized; (iii) at the end, a full diagnostic of all critical structures of reaction **1** with **2a–c** are studied.

#### 3.1. Analysis of the Electronic Properties of Addends and Their Intermolecular Interactions according to CDFT

The CDFT is a very important tool to understand the reactivity in polar cycloadditions. The CDFT indices were calculated in the gas phase according to the B3LYP/6-31G(d) theory level because it was used to define the electrophilicity and nucleophilicity scales. The global reactivity indices, namely, electronic chemical potential  $\mu$ , chemical hardness  $\eta$ , global electrophilicity  $\omega$  and global nucleophilicity  $N$ , for the reagents involved in these 32CA reactions are given in Table 1.

**Table 1.** Electronic chemical potential  $\mu$ , chemical hardness  $\eta$ , global electrophilicity  $\omega$  and nucleophilicity  $N$ , in eV, for the studied reagents, calculated based on B3LYP/6-31G(d) theory level.

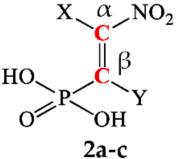
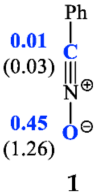
	$\mu$	$\eta$	$\omega$	$N$
<b>1</b>	−3.83	5.02	1.46	2.78
<b>2a</b>	−5.54	5.15	2.98	1.00
<b>2b</b>	−6.01	4.90	3.68	0.66
<b>2c</b>	−6.09	4.79	3.87	0.64

The electronic chemical potential  $\mu$  of benzonitrile N-oxide **1**, −3.83 eV, is significantly lower than for  $\beta$ -phosphorylated analogues of nitroethenes **2a–c** (see Table 1). It means that while along the 32CA reactions between TAC **1** and nitroethenes **2a–c**, the flux of the electron density will take place from benzonitrile N-oxide **1** to these nitroethenes **2a–c**.

The global electrophilicity  $\omega$  and the global nucleophilicity  $N$  indexes for benzonitrile N-oxide **1** are respectively 1.46 and 2.78 eV (see Table 1). Based on the electrophilicity [48,49] and nucleophilicity [50] scale, TAC **1** can be classified as a moderate electrophile and a moderate nucleophile. According to the same scale,  $\beta$ -phosphorylated analogues of nitroethenes **2a–c** can be classified as strong electrophiles ( $\omega = 2.98–3.87$  eV) and marginal nucleophiles ( $N = 0.64–1.00$  eV). What is more, it is worth noting that the introduction of a cyano group to nitroalkene **2a** both directly at carbon atom of nitro group ( $C_\alpha$ ) and at the same atom as the phosphoryl group ( $C_\beta$ ) causes a significant increase in the values of global electrophilicity (by approximately 0.7–0.8 eV), while we can see a decrease of the values of global nucleophilicity (by approximately 0.3–0.4 eV) (Table 1).

To summarize, in the analyzed [3+2] cycloaddition reactions benzonitrile N-oxide **1** will participate as nucleophile (electron donor), while  $\beta$ -phosphorylated analogues of nitroethenes **2a–c** will perform a role of electrophile (electron acceptor). Moreover, according to one of the fundamental MEDT rules, the interaction between the tested components should be evidently classified as polar processes [54]. Therefore, for analyzed processes non-polar mechanisms such as biradicaloidal one-step or stepwise biradical are not possible.

The regioselectivity of a polar reaction involving the participation of non-symmetric reagents can be specified through interaction between the most electrophilic centre for the electrophile component and the most nucleophilic centre for the nucleophile component. Due to this, the Parr functions were the most exact and discerning implements that enabled the study of the local parameters of the reaction [55]. Therefore, the electrophilic  $P_k^+$  and nucleophilic  $P_k^-$  Parr functions of addends were analyzed to determine the most nucleophilic and the most electrophilic centres for the analyzed addends (see Figure 1).

	X	Y	$P_{C\alpha^+}(\omega_{C\alpha})$	$P_{C\beta^+}(\omega_{C\beta})$		
	<b>2a</b>	H	H	<b>0.14</b> (0.42)	<b>0.32</b> (0.96)	
	<b>2b</b>	CN	H	<b>0.08</b> (0.30)	<b>0.49</b> (1.81)	
	<b>2c</b>	H	CN	<b>0.26</b> (1.01)	<b>0.25</b> (0.97)	

**Figure 1.** The local electronic properties for benzonitrile N-oxide **1** and  $\beta$ -phosphorylated analogues of nitroethenes **2a–c**. The nucleophilic  $P_k^-$  is given in blue and the electrophilic  $P_k^+$  is given in red. The indexes of local nucleophilicity  $N_k$  and local electrophilicity  $\omega_k$  are given in brackets.

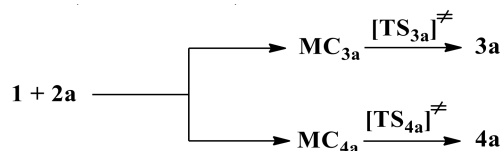
Studies of the nucleophilic Parr functions for benzonitrile N-oxide **1** show that the oxygen atom is the most nucleophilic centre of this species presenting the maximum value,  $P_{O^-} = 0.45$  eV. For this atom, the value of the local nucleophilicity  $N_k$  index is  $N_O = 1.26$  eV (see Figure 1).

In turn, the analysis of the electrophilic  $P_k^+$  Parr functions of  $\beta$ -phosphorylated analogues of nitroethenes **2a** and **2b** shows that for these molecules the most electrophilic centre of this species are the  $C_\beta$  carbons, presenting the maximum values in the range  $P_{C\beta^+} = 0.32$ – $0.49$  eV. At these atoms, the values of the local electrophilicity  $\omega_{C\beta}$  indexes are in the range  $\omega_{C\beta} = 0.96$ – $1.81$  eV (see Figure 1). In turn, the electrophilic  $P_k^+$  Parr functions for **2c** are practically identical, both for the atom  $C_\alpha$ ,  $P_{C\alpha^+} = 0.26$  eV, and  $C_\beta$ ,  $P_{C\beta^+} = 0.25$  eV. The values of the local electrophilicity of these centres are, respectively,  $1.01$  ( $\omega_{C\alpha}$ ) and  $0.97$  ( $\omega_{C\beta}$ ) eV (see Figure 1).

According to CDFT theory, the described interactions show that for the [3+2] cycloadditions between **1** and **2a–b**, the more preferred reaction channel is forming 4-nitro-substituted  $\Delta^2$ -isoxazolines **3a–b**, while for the process of **1** with **2c** both regioisomers of 4-nitro- and 5-nitro-substituted  $\Delta^2$ -isoxazolines (respectively **3c** and **4c**) can be formed with the similar probability.

### 3.2. Reaction Profiles of 32CA between Benzonitrile N-Oxide and $\beta$ -Phosphorylated Analogues of Nitroethenes

Secondly, the 32CA processes between benzonitrile N-oxide **1** and  $\beta$ -phosphorylated nitroethenes **2a–c** were studied. The quantum-chemical calculation was performed according to the functional M062X with the 6-31+G(d) basis set. Stationary points corresponding to the existence of molecular complexes (MCs) and transition complexes (TSs) were found on both reaction paths, between minimums for the addends and the products of reaction (see Scheme 2).



**Scheme 2.** 32CA reaction between benzonitrile N-oxide **1** and  $\beta$ -phosphoryl nitroethene **2a**.

Quantum-chemical calculations have shown that the reaction between **1** and **2a** in toluene ( $\epsilon = 2.38$ ) as a solvent leads to molecular complexes MC at the first reaction stage for both of the reaction channels. MCs are created without necessity of crossing an activation barrier. Due to this fact, we can observe a significant drop in an enthalpy, as well as a small reduction of entropy. This, in turn, eliminates the appearance of MC structures as stable intermediates due to thermodynamic rules considered at room temperature. A similar type of intermediate was also localized in the 32CAs containing cyano analogues  $\beta$ -phosphorylated nitroethenes **2b** and **2c** (see Table S1).

Further conversion of reaction system of **1** + **2a** alongside the process path, irrespective of the 32CA channel, leads in the next stage to the transition state TS. It is confirmed by

IRC analysis. The appearance of a transition state was established by the presence of one imaginary eigenvalue in the Hessian and it is associated with increase of the Gibbs free energy of the process by 23 kcal in a relation with the creating of **3a** and about 24 kcal/mol in the case of creating of **4a** (see Table S1). Based on the given values, it can be concluded that both of reaction channels lead to 4-nitro- and 5-substituted adducts (respectively **3a** and **4a**) and both should be considered as kinetically allowed (see Figure 2). Moreover, the more favoured reaction channel is a creation of 4-substituted  $\Delta^2$ -isoxazoline **3a**. This conclusion corresponds well with the results of the intermolecular interactions of addends according to CDFT discussed above (see Figure 1).

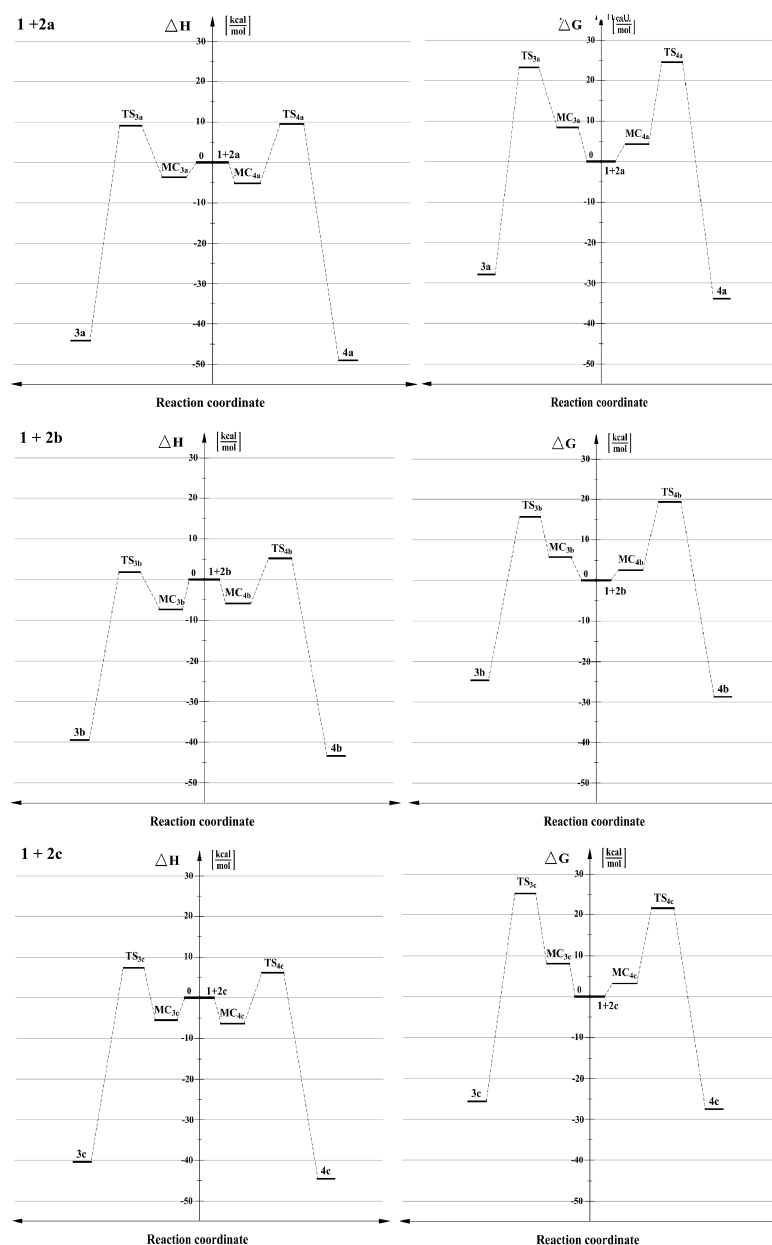


**Figure 2.** Energy profiles for the 32CA between benzonitrile N-oxide **1** and  $\beta$ -phosphorylated analogues of nitroethenes **2a–c**, in toluene, according to M062X/6-31+G(d) calculations (PCM).

When more polar solvents, such as nitromethane ( $\epsilon = 36.56$ ) solution (see Table S1), were included as dielectric media in DFT calculations, the reaction profiles did not change qualitatively, but they did change quantitatively to a small extent. In particular, the MCs in all the energy profiles were slightly flat and all activation barriers were significantly higher.

Nevertheless, the order of the process channels priority based on kinetics, in nitromethane, which is characterized as a greatly polar solvent, was identical as analyzed once in toluene solution (see Figure 2).

When the structure of **2a** is modified by replacement of  $\alpha$ -hydrogen within nitrovinyl moiety by a cyano group, the profile of the considered reaction channel **1** + **2b** does not change qualitatively. Even so, some transformations occur in a quantitative way (see Table S1). In particular, activation barriers in both channels are lower than analyzed above 32CA. It is caused by the presence of the two electron-withdrawing (EWG) groups—nitro and cyano—directly situated at the same  $\alpha$ -carbon in nitroalkene **2b**. These groups have an impact for molecule **2b**, causing significant influence of electrophilicity on  $\beta$ -carbon (see Figure 1 and Table S1). Also, for the analyzed cycloaddition **1** + **2b**, forming of adducts **3b** and **4b** should be considered as kinetically allowed. Moreover, the more favoured reaction channel is the formation of 4-substituted  $\Delta^2$ -isoxazoline **3b**. The above observations are also similar for nitromethane as a solvent. All presented results correlate well with the analysis of the intermolecular interactions of addends according to CDFT (see Figure 1).

In turn, if the structure of **2a** is altered by the replacement of  $\beta$ -hydrogen within nitrovinyl moiety by a cyano group, the profile of the considered reaction channel **1** + **2c** does change both qualitatively as well as quantitatively (see Table S1). In particular, the values of the activation barrier are very similar in comparison with the model reaction **1** + **2a**. Furthermore, for analyzed cycloaddition **1** + **2c**, the forming of adducts **3c** and **4c** should be considered as kinetically allowed; however, in contrast to 32CA analyzed above, the more favoured reaction channel is a creation of 5-substituted  $\Delta^2$ -isoxazoline **4c**, independently of a solvent. The change of regioisomerism for the analyzed cycloaddition **1** + **2c** is caused by the occurrence of a cyano group in a  $\beta$ -position of nitroalkene **2c**. The substituent interacts on  $\alpha$ -atom of carbon in **2c**, increasing the value of electrophilicity (see Figure 1 and Table S1). These observations correlate well with the analysis of the intermolecular interaction of addends according to CDFT (see Figure 1).

### 3.3. Critical Structures for Reaction of 32CA between Benzonitrile N-Oxide and $\beta$ -Phosphorylated Nitroethenes

#### 3.3.1. Pre-Reaction Molecular Complexes (MC)

As noted in previous paragraphs, the first stage in each of the 32CA processes considered in toluene solution ( $\epsilon = 2.38$ ) is always the formation of a molecular complex MC (respectively  $MC_{3a}$  and  $MC_{4a}$  for competitive reaction channels) (see Figure 3 and Table S2). Analysis of the structural aspects of each MC have shown that the bond lengths for O1–N2, N2–C3 and C4–C5 were practically identical as analogous lengths in the individual molecules. What is more, within MCs distances between reaction centres (respectively C3–C4 and C5–O1) were about a few Å, still remaining far outside the range typical for  $r$  bonds in transition states. Also, in the MCs, the orientations of the reaction centres compared to each other are not the same as they are in the final products. Additionally, based on the GEDT values (0.0 e), none of the MCs are charge-transfer complexes. Change of the solvent to the slightly more polar nitromethane ( $\epsilon = 36.56$ ) does not cause significant changes in the nature of the molecular complexes (see Figure 3 and Table S2).

#### 3.3.2. Transition States (TS)

Conversion of the MC into the required adduct was always found to occur via a single TS (respectively  $TS_{3a}$  and  $TS_{4a}$  for competitive reaction channels) (see Figure 3 and Table S2). Within TSs, the C3–C4 and C5–O1 atomic distances have been significantly shortened, compared to the corresponding distances within the MC. The nature of the TSs depends to some extent on the relative orientations of its substructures. In particular, for cycloaddition with benzonitrile N-oxide **1** with  $\beta$ -phosphoryl nitroethene **2a** in toluene solution ( $\epsilon = 2.38$ ), for the  $TS_{3a}$  obtained in the reaction channel which ultimately yields 4-nitro-substituted  $\Delta^2$ -isoxazoline **3a**, the extent of C3–C4 and C5–O1 forming new bonds is rather similar ( $l = 0.477$  and  $0.450$ , respectively). In turn, within the competitive  $TS_{4a}$ ,

obtained in the reaction channel which ultimately yields 5-nitro-substituted  $\Delta^2$ -isoxazoline **4a**, the stage of advancement C5–O1 sigma bond is 0.442, while the C3–C4 sigma bond is formed not much earlier, 0.551. It seems that, for the more favoured reaction channel in a kinetic point of view, TS<sub>3a</sub> is more synchronic. Likewise, both TSs exhibit evidently [54] polar nature, which is confirmed in the GEDT index value (see Table S1). In particular, more asynchronous TS<sub>4a</sub> is connected with the higher value of GEDT.

In the case of a similar cycloaddition between **1** and  $\beta$ -phosphorylated  $\alpha$ -cyanonitroethene **2b**, in the same reaction medium (toluene), the level of asynchronicity for both TSs changes significantly. In particular, for the TS<sub>3b</sub> received in the reaction channel which finally yields **3b**, the stage of advancement C5–O1 sigma bond increases ( $l = 0.681$ ), while for the C3–C4 sigma bond the stage of advancement is reduced ( $l = 0.426$ ), in comparison to a model reaction **1** + **2a** (see Table S2). Similarly, for the competitive TS<sub>B</sub>, obtained in the reaction channel which ultimately yields **4b**, the stage of advancement C5–O1 sigma bond is reduced ( $l = 0.425$ ), whilst for the C3–C4 sigma bond the stage of advancement increases ( $l = 0.682$ ), in comparison to a model reaction **1** + **2a** (see Table S2). A much higher stage of advancement of the C5–O1 sigma bond for reaction channel **3b** and C3–C4 sigma bond for reaction channel **4b** is caused by the presence of a cyano group in  $\alpha$ -carbon in nitroalkene **2b**, causing a significant influence of electrophilicity on carbon in  $\beta$  position. For reaction **1** + **2b**, both TSs present a similar synchronic and are characterized by a more polar nature, in comparison to 32CA analyzed above (see GEDT in Table S2). The slightly higher values of GEDT are caused by the presence of an additional EWG and associated with it, increasing asynchronicity when creating new sigma bonds.

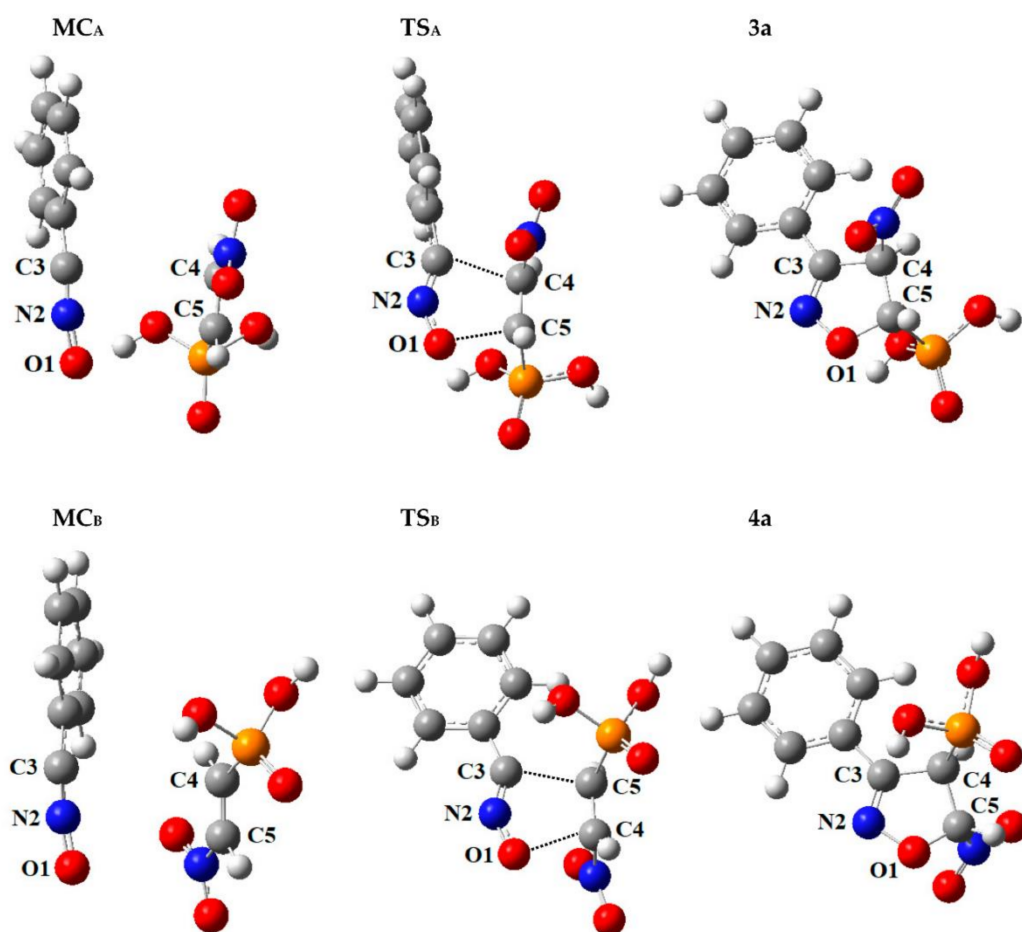


**Figure 3.** Critical structures for the reaction of 32CA between benzonitrile N-oxide **1** and  $\beta$ -phosphoryl nitroethene **2a**, in toluene, according to M062X/6-31+G(d) calculations (PCM).

The clear influence of the existence of a cyano group on the structure of TS can be also observed for cycloaddition between **1** and  $\beta$ -phosphorylated  $\beta$ -cyanonitroethene **2c**, in toluene. For the analyzed case, the asynchronicity level of both TSs is similar to above analyzed 32CA and simultaneously higher in comparison to a model reaction **1** + **2a** (see Table S2). In particular, for the TS<sub>3c</sub> localized within the reaction channel which ultimately yields **3c**, the stage of advancement the C3–C4 sigma bond ( $l = 0.579$ ) is higher than for the C5–O1 sigma bond ( $l = 0.517$ ); however, the difference is not very significant (see Table S2). On the other hand, for the competitive TS<sub>4c</sub>, obtained in the reaction channel which ultimately yields **4c**, the higher stage of advancement is observed for the C5–O1 sigma bond ( $l = 0.609$ ), than the C3–C4 sigma bond ( $l = 0.469$ ). It seems that, for the more favoured reaction channel in a kinetic point of view, TS<sub>4c</sub> is more asynchronous. Also, both TS<sub>3c</sub> and TS<sub>4c</sub> are characterized by a similar polar nature, in comparison to 32CA analyzed above, except that for a more asynchronous TS<sub>4c</sub> the value of GEDT is significantly higher (see Table S2). In this case, a much higher stage of advancement of the C3–C4 sigma bond for reaction channel **3c** and the C5–O1 sigma bond for reaction channel **4c** is also caused by the presence of a cyano group in  $\beta$ -carbon in nitroalkene **2c**. It causes an influence of electrophilicity on carbon in  $\alpha$  position. However, this effect is smaller than in the previously analyzed 32CA due to the presence of a nitro group in  $\alpha$  position.

Due to the use of a strong polar medium, such as nitromethane ( $\epsilon = 36.56$ ) in the reaction medium, the main parameters of all analyzed structures are not changed significantly (see Table S2). In particular, for the structure of all TSs the GEDT values increase, which exhibits their more polar nature.

#### 4. Conclusions

The reactions of [3+2] cycloaddition between benzonitrile N-oxide **1** and  $\beta$ -phosphorylated analogues of nitroethenes **2a–c** have been studied according to M062X/6-31+G(d) theory level. Received results are confirmed by the analysis combination of the Conceptual Density Functional Theory reactivity indices at the ground state of the addends and analyzed according to the reaction profiles and study of the critical structures located on the reaction paths.

The analysis of the reactivity shows that benzonitrile N-oxide **1** can be classified both as a moderate electrophile and moderate nucleophile. The mentioned analysis has also shown that  $\beta$ -phosphorylated analogues of nitroethenes **2a–c** can be classified as a strong electrophiles and marginal nucleophiles. Moreover, for a model reaction **1** + **2a** the more favored reaction path is forming 4-nitro-substituted  $\Delta^2$ -isoxazoline **3a**. The same preference can be observed for cycloaddition **1** + **2b**, while for reaction of **1** + **2c** both reaction channels are possible to the same extent. It is caused by the presence of a cyano group in different positions of nitrovinyl moiety. What is more, the interaction between the tested components should be evidently classified as polar processes.

The analysis of the reaction profiles for all cycloadditions indicates that the processes between **1** and **2a–c** should be regarded as polar, except one-step processes. All attempts for the localization of competitive channels leads to zwitterionic intermediates were not successful. It should be underlined at this point that estimated parameters of the activation suggest that the synthesis of the expected phosphorylated nitroisoxazolines is fully allowed with good regioselectivity even under mild conditions. Finally, the significant influence on the kinetic aspects as well as predicted regioselectivity exhibit the presence of EWG at the  $\alpha$ -position at nitrovinyl moiety.

**Supplementary Materials:** The following are available online at <https://www.mdpi.com/2673-401X/2/1/3/s1>.

**Author Contributions:** Conceptualization, K.K. and K.Z.; methodology, K.K.; investigation, K.K., K.Z.; resources, K.K. and K.Z.; data curation, K.K.; writing—original draft preparation, K.K.; writing—review and editing, K.K. and K.Z.; visualization, K.K. and K.Z.; supervision, K.K.; project administration, K.K. and K.Z. All authors have read and agreed to the published version of the manuscript.

**Funding:** This research received no external funding.

**Institutional Review Board Statement:** Not applicable.

**Informed Consent Statement:** Not applicable.

**Data Availability Statement:** The data presented in this study are available on request from the corresponding author.

**Acknowledgments:** All calculations reported in this paper were performed on “Prometheus” supercomputer cluster in the CYFRONET computational centre in Cracow. Support of this research is gratefully acknowledged.

**Conflicts of Interest:** The authors declare no conflict of interest.

## References

1. Huisgen, R. 1,3-Dipolare Cycloadditionen Rückschau und Ausblick. *Angew. Chem. Int. Ed.* **1963**, *75*, 604–637. [[CrossRef](#)]
2. Jasiński, R.; Zmigrodzka, M.; Dresler, E.; Kula, K. A full regio- and stereoselective synthesis of 4-nitroisoxazolidines via stepwise [3+2] cycloaddition reactions between (Z)-C-(9-anthryl)-N-arylnitrones and (E)-3,3,3-trichloro-1-nitroprop-1-ene: Comprehensive experimental and theoretical study. *J. Heterocycl. Chem.* **2017**, *54*, 3314–3320. [[CrossRef](#)]
3. Łapczuk-Krygier, A.; Kačka-Zych, A.; Kula, K. Recent progress in the field of cycloaddition reactions involving conjugated nitroalkenes. *Curr. Chem. Lett.* **2019**, *8*, 13–38. [[CrossRef](#)]
4. Fryzlewicz, A.; Łapczuk-Krygier, A.; Kula, K.; Demchuk, O.M.; Dresler, E.; Jasiński, R. Regio- and stereoselective synthesis of nitro-functionalized analogs of nicotine. *Chem. Heterocycl. Compd.* **2020**, *56*, 120–122. [[CrossRef](#)]
5. Martina, K.; Tagliapietra, S.; Veselov, V.V.; Cravotto, G. Green Protocols in Heterocycle Syntheses via 1,3-Dipolar Cycloadditions. *Front. Chem.* **2019**, *7*, 95. [[CrossRef](#)] [[PubMed](#)]
6. Zhang, P.Z.; Li, X.L.; Chen, H.; Li, Y.N.; Wang, R. The synthesis and biological activity of novel spiro-isoxazoline C-disaccharides based on 1,3-dipolar cycloaddition of exo-glycals and sugar nitrile oxides. *Tetrahedron Lett.* **2007**, *48*, 7813–7816. [[CrossRef](#)]
7. Jasinski, R.; Dresler, E. On the Question of Zwitterionic Intermediates in the [3+2] Cycloaddition Reactions: A Critical Review. *Organics* **2020**, *7*, 5. [[CrossRef](#)]
8. Kula, K.; Łapczuk-Krygier, A. A DFT computational study on the [3+2] cycloaddition between parent thionitronone and nitroethene. *Curr. Chem. Lett.* **2018**, *7*, 27–34. [[CrossRef](#)]
9. Kula, K.; Dobosz, J.; Jasiński, R.; Kačka-Zych, A.; Łapczuk-Krygier, A.; Mirosław, B.; Demchuk, O.M. [3+2] Cycloaddition of diaryldiazomethanes with (E)-3,3,3-trichloro-1-nitroprop-1-ene: An experimental, theoretical and structural study. *J. Mol. Struct.* **2020**, *1203*, 127473. [[CrossRef](#)]
10. Huisgen, R. 1,3-Dipolar Cycloadditions. Past and Future. *Angew. Chem. Int. Ed.* **1963**, *2*, 565–598. [[CrossRef](#)]
11. Jeddeloh, M.R.; Holden, J.B.; Nouri, D.H.; Kurth, M.J. A Library of 3-aryl-4,5-dihydroisoxazole-5-carboxamides. *J. Comb. Chem.* **2007**, *9*, 1041–1045. [[CrossRef](#)]
12. Quadrelli, P.; Martinez, N.V.; Scrocchi, R.; Corsaro, A.; Pistarà, V. Syntheses of Isoxazoline-Carbocyclic Nucleosides and Their Antiviral Evaluation: A Standard Protocol. *Sci. World J.* **2014**, *2014*, 492178. [[CrossRef](#)] [[PubMed](#)]
13. Znati, M.; Debbabi, M.; Romdhane, A.; Ben Jannet, H.; Bouajila, J. Synthesis of new anticancer and anti-inflammatory isoxazolines and aziridines from the natural (-)-deltoin. *J. Pharm. Pharmacol.* **2018**, *70*, 1700–1712. [[CrossRef](#)] [[PubMed](#)]
14. Filial, I.; Bouajila, J.; Znati, M.; Bousejra-El Garah, F.; Ben Jannet, H. Synthesis of new isoxazoline derivatives from harmine and evaluation of their anti-Alzheimer, anti-cancer and anti-inflammatory activities. *J. Enzyme Inhibit. Med. Chem.* **2014**, *30*, 371–376. [[CrossRef](#)]
15. Saravanan, G.; Alagarsamy, V.; Dineshkumar, P. Synthesis, analgesic, anti-inflammatory and in vitro antimicrobial activities of some novel isoxazole coupled quinazolin-4(3H)-one derivatives. *Arch. Pharm. Res.* **2013**. [[CrossRef](#)]
16. Sharifi, B.; Zade, B.G.; Zoladl, M.; Najafi, D.S.; Ghafarian, S.; Hamid, R.; Hashemi, M.; Abad, N. Side effects of risperidone. *Life Sci. J.* **2012**, *9*, 1463–1467. [[CrossRef](#)]
17. Barceló, M.; Raviña, E.; Masaguer, C.F.; Domínguez, E.; Areias, F.M.; Brea, J.; Loza, M.I. Synthesis and binding affinity of new pyrazole and isoxazole derivatives as potential atypical antipsychotics. *Bioorg. Med. Chem. Lett.* **2007**, *17*, 4873–4877. [[CrossRef](#)]
18. Pinho e Melo, T.M.V.D. Recent Advances on the Synthesis and Reactivity of Isoxazoles. *Curr. Org. Chem.* **2005**, *9*, 925–958. [[CrossRef](#)]
19. Kanemasa, S.; Tsuge, O. Recent advances in synthetic applications of nitrile oxide cycloaddition. *Heterocycles* **1990**, *30*, 719–736. [[CrossRef](#)]
20. Sewald, N. Synthetic Routes towards Enantiomerically Pure  $\beta$ -Amino Acids. *Angew. Chem. Int. Ed.* **2003**, *42*, 5794–5795. [[CrossRef](#)]
21. Harada, K.; Kaji, E.; Takahashi, K.; Zen, S. Ring Transformation of 2-Isoxazoline 2-Oxides by Lewis Acids. *Rev. Heteroatom Chem.* **1997**, *16*, 171–195. [[CrossRef](#)]
22. Ono, N. *The Nitro Group in Organic Synthesis*; Wiley-VSH: New York, NY, USA, 2001. [[CrossRef](#)]

23. Padwa, A.; Pearson, W.H. *Synthetic Applications of 1,3-Dipolar Cycloaddition Chemistry Toward Heterocycles and Natural Products*; John Wiley & Sons: New York, NY, USA, 2002. [\[CrossRef\]](#)
24. Boguszewska-Czubarra, A.; Kula, K.; Wnorowski, A.; Biernasiuk, A.; Popiolek, P.; Miodowski, D.; Demchuk, O.M.; Jasiński, R. Novel functionalized  $\beta$ -nitrostyrenes: Promising candidates for new antibacterial drugs. *Saudi Pharm. J.* **2019**, *27*, 593–601. [\[CrossRef\]](#)
25. Yan-Mei, L.; Ying-Wu, Y.; Yu-Fen, Z. Phosphoryl group participation leads to peptide formation from N-phosphorylamino acids. *Int. J. Peptide Protein Res.* **1992**, *39*, 375–381. [\[CrossRef\]](#)
26. Nalwa, H.S. *Handbook of Surfaces and Interfaces of Materials*; Academic Press: Los Angeles, CA, USA, 2001.
27. Ram, V.J.; Sethi, A.; Nath, M.; Pratap, R. *The Chemistry of Heterocycles*; Elsevier: Amsterdam, The Netherlands, 2019. [\[CrossRef\]](#)
28. Mersbergen, D.; Wijnen, J.W.; Engberts, J.B.F.N. 1,3-Dipolar Cycloadditions of Benzonitrile Oxide with Various Dipolarophiles in Aqueous Solutions. A Kinetic Study. *J. Org. Chem.* **1998**, *63*, 8801–8805. [\[CrossRef\]](#)
29. Jasiński, R.; Jasińska, E.; Dresler, E. A DFT computational study of the molecular mechanism of [3+2] cycloaddition reactions between nitroethene and benzonitrile N-oxides. *J. Mol. Model.* **2017**, *23*, 13. [\[CrossRef\]](#) [\[PubMed\]](#)
30. Domingo, L.R.; Emamian, S.; Salami, M.; Ríos-Gutiérrez, M. Understanding the molecular mechanism of the [3+2] cycloaddition reaction of benzonitrile oxide toward electron-rich N-vinylpyrrole: A DFT study. *J. Phys. Org. Chem.* **2016**, *29*, 368–376. [\[CrossRef\]](#)
31. Domingo, L.R.; Ríos Gutiérrez, M.; Castellanos Soriano, J. Understanding the Origin of the Regioselectivity in Non-Polar [3+2] Cycloaddition Reactions through the Molecular Electron Density Theory. *Organics* **2020**, *1*, 3. [\[CrossRef\]](#)
32. Jasiński, R.; Ziółkowska, M.; Demchuk, O.M.; Maziarka, A. Regio- and stereoselectivity of polar [2+3] cycloaddition reactions between (Z)-C-(3,4,5-trimethoxyphenyl)-N-methylnitron and selected (E)-2-substituted nitroethenes. *Cent. Eur. J. Chem.* **2014**, *12*, 586–593. [\[CrossRef\]](#)
33. Jasiński, R. Competition between one-step and two-step mechanism in polar [3+2] cycloadditions of (Z)-C-(3,4,5-trimethoxyphenyl)-N-methyl-nitron with (Z)-2-EWG-1-bromo-1-nitroethenes. *Comput. Theor. Chem.* **2018**, *1125*, 77–85. [\[CrossRef\]](#)
34. Frisch, M.J.; Trucks, G.W.; Schlegel, H.B.; Scuseria, G.E.; Robb, M.A.; Cheeseman, J.R.; Scalmani, G.; Barone, V.; Petersson, G.A.; Nakatsuji, H.; et al. *Gaussian 09 Rev. A.02*; Gaussian, Inc.: Wallingford, CT, USA, 2016.
35. Jasiński, R. A new insight on the molecular mechanism of the reaction between (Z)-C,N-diphenylnitron and 1,2-bismethylene-3,3,4,4,5,5-hexamethylcyclopentane. *J. Mol. Graph. Model.* **2020**, *94*, 107461. [\[CrossRef\]](#)
36. Kačka-Zych, A. Participation of Phosphorylated Analogues of Nitroethene in Diels–Alder Reactions with Anthracene: A Molecular Electron Density Theory Study and Mechanistic Aspect. *Organics* **2020**, *1*, 4. [\[CrossRef\]](#)
37. Kula, K.; Zawadzińska, K. Local nucleophile-electrophile interactions in [3+2] cycloaddition reactions between benzonitrile N-oxide and selected conjugated nitroalkenes in the light of MEDT computational study. *Curr. Chem. Lett.* **2021**, *10*, 9–16. [\[CrossRef\]](#)
38. Stephens, P.; Devlin, F.J.; Chabalowski, C.F.; Frisch, M.J. Ab Initio Calculation of Vibrational Absorption and Circular Dichroism Spectra Using Density Functional Force Fields. *J. Phys. Chem.* **1994**, *98*, 11623–11627. [\[CrossRef\]](#)
39. Domingo, L.R.; Kula, K.; Ríos-Gutiérrez, M. Unveiling the Reactivity of Cyclic Azomethine Ylides in [3+2] Cycloaddition Reactions within the Molecular Electron Density Theory. *Eur. J. Org. Chem.* **2020**, 5938–5948. [\[CrossRef\]](#)
40. Schlegel, H.B. Optimization of equilibrium geometries and transition structures. *J. Comput. Chem.* **1982**, *3*, 214–218. [\[CrossRef\]](#)
41. Schlegel, H.B. *Modern Electronic Structure Theory*; Yarkony, D.R., Ed.; World Scientific Publishing: Singapore, 1994.
42. Fukui, K. Formulation of the reaction coordinate. *J. Phys. Chem.* **1970**, *74*, 4161–4163. [\[CrossRef\]](#)
43. Tapia, O. Solvent Effect Theories: Quantum and Classical Formalism and their Applications in Chemistry and Biochemistry. *J. Math. Chem.* **1992**, *10*, 131–181. [\[CrossRef\]](#)
44. Tomasi, J.; Perisco, M. Molecular Interactions in Solution: An Overview of Methods Based on Continuous Distributions of the Solvent. *Chem. Rev.* **1994**, *94*, 2017–2094. [\[CrossRef\]](#)
45. Cossi, M.; Barone, V.; Cammi, R.; Tomasi, J. Ab initio study of solvated molecules: A new implementation of the polarizable continuum model. *Chem. Phys. Chem.* **1996**, *225*, 327–335. [\[CrossRef\]](#)
46. Domingo, L.R. A New C-C bond formation model based on the quantum chemical topology of electron density. *RSC Adv.* **2014**, *4*, 32415–32428. [\[CrossRef\]](#)
47. Mloston, G.; Jasiński, R.; Kula, K.; Heimgartner, H. A DFT Study on the Barton-Kellogg Reaction—The Molecular Mechanism of the Formation of Thiiranes in the Reaction between Diphenyldiazomethane and Diaryl Thioketones. *Eur. J. Org. Chem.* **2020**, 176–182. [\[CrossRef\]](#)
48. Parr, R.G.; Szentpaly, L.V.; Liu, S. Electrophilicity Index. *J. Am. Chem. Soc.* **1999**, *121*, 1922–1924. [\[CrossRef\]](#)
49. Domingo, L.R.; Ríos-Gutiérrez, M.; Pérez, P. Applications of the Conceptual Density Functional Theory Indices to Organic Chemistry Reactivity. *Molecules* **2016**, *21*, 748. [\[CrossRef\]](#)
50. Pérez, P.; Domingo, L.R.; Duque-Noreña, M.; Chamorro, E. A condensed-to-atom nucleophilicity index. An application to the director effects on the electrophilic aromatic substitutions. *J. Mol. Struct.* **2009**, *895*, 86–91. [\[CrossRef\]](#)
51. Grellings, P.; De Proft, F.; Langenaeker, W. Conceptual Density Functional Theory. *Chem. Rev.* **2003**, *103*, 1793–1874. [\[CrossRef\]](#)
52. Pérez, P.; Domingo, L.R.; Aurell, M.J.; Contreras, R. Quantitative characterization of the global electrophilicity pattern of some reagents involved in 1,3-dipolar cycloaddition reactions. *Tetrahedron* **2003**, *59*, 3117–3125. [\[CrossRef\]](#)
53. Domingo, L.R.; Pérez, P.; Saez, J.A. Understanding the local reactivity in polar organic reactions through electrophilic and nucleophilic Parr functions. *RSC Adv.* **2013**, *3*, 1486–1494. [\[CrossRef\]](#)

- 
54. Domingo, L.R.; Saez, J.A. Understanding the mechanism of polar Diels-Alder reactions. *Org. Biomol. Chem.* **2009**, *7*, 3576–3583. [[CrossRef](#)]
  55. Domingo, L.R.; Ríos-Gutiérrez, M. On the nature of organic electron density transfer complexes within molecular electron density theory. *Org. Biomol. Chem.* **2019**, *17*, 6478–6488. [[CrossRef](#)]